Presented at the E-MRS Spring Meeting, Strasbourg (F), june 2003
Accepted for publication in Thin Solid Films, September 2003

CHARACTERIZATION OF DEEP DEFECTS IN CDS/CDTE THIN FILM SOLAR CELLS USING DEEP LEVEL TRANSIENT SPECTROSCOPY

J. Versluys*(1), P. Clauws(1), P. Nollet(2), S. Degrave(2) and M. Burgelman(2)

(1)Ghent University, Department of Solid State Sciences, Krijgslaan 281 S1, B-9000 Gent, Belgium
(2)Ghent University, Electronics and Information Systems (ELIS), St.-Pietersnieuwstraat 41, B-9000 Gent, Belgium

Abstract

The presence of deep defects in CdS/CdTe thin film solar cells strongly affects the electrical properties and as a result the performance of the cells. Therefore it is desirable to understand the role of these defect states.
This paper describes the detection of electron traps in CdS/CdTe thin film solar cells using Deep Level Transient Spectroscopy. Two series of samples with a different activation step (activation in air versus activation in vacuum) are compared. Electrical injection DLTS uses an electrical pulse to inject electrons in the CdTe. This way a new electron trap could be characterized at 0.44eV below conduction band in the air activated cells. Optical DLTS uses an optical laser pulse (λ=635nm) to create minority carriers. In this case minority traps are found in both kinds of samples. In the air activated cells two closely spaced defects are detected (0.44 and 0.42 eV below conduction band) with concentrations of a few percent of the background concentration. In the vacuum activated cells a broad band is detected. However not fully characterized, it is located at about 0.4eV below conduction band.
Using the DLTS results, simulations were performed to explain the forward JV-characteristics of the solar cells. These simulations are in close agreement with the experimental results if the concentrations of the deep traps are taken sufficiently high.

Keywords: CdTe, solar cell, deep level, DLTS
PACS: 71.55.-I, 72.40.+w

1. Introduction

* Corresponding author. Tel. +32 9 2644364; Fax. +32 9 2644996; E-mail: jorg.versluys@UGent.be

Production of large CdS/CdTe thin film solar cell modules is still limited by the low efficiency of the photovoltaic process compared with silicon based solar cells. Although CdS/CdTe solar cells can reach efficiencies up to 27% [1], large commercial modules only reach values of about 9% [2]. One of the major reasons for this poor performance is the presence of deep defects in the CdTe absorber layer. These defects can capture the charge carriers generated by the photovoltaic energy conversion, resulting in a decrease of output current, a loss in the open circuit voltage and thus a lowering of the cell's efficiency. In order to produce high efficiency CdS/CdTe thin film solar cells knowledge of the origin and nature of these defects is necessary.
In a previous paper [3] we already discussed the detection of deep defects using Deep Level Transient Spectroscopy and Admittance Spectroscopy. Furthermore the influence of the activation ambient during the production of the solar cell on the cell's performance was investigated [4] . In this paper we discuss the results acquired by electrical injection DLTS and optical DLTS. We also try to explain the current characteristics of the cells by taking into account the presence of the detected deep levels.

2. Experimental

Complete CdS/CdTe thin film solar cells were supplied by Antec Technology GmbH. More details about the configuration as well as the DLTS setup can be found in [3]. In order to detect minority traps (normal DLTS only characterizes majority traps, i.e. hole traps in p – type CdTe), electrical injection DLTS (inj-DLTS) as well as optical DTLS (O-DLTS) were used. In inj-DLTS minority carriers (electrons in CdTe) are injected in the diode by switching it in forward polarisation during pulsing. In O-DLTS holes and electrons are generated with an optical pulse, while the sample is kept at a constant reverse bias throughout the measurement. Light, originating from a laser diode with $\lambda = 635$nm, is directed towards the CdTe layer through the glass, the front contact and the CdS layer, resulting in the creation of electron hole pairs. Because of the high absorption of these photons in the CdTe layer ($\alpha^{-1} \approx 0.25\mu$m) [8], only about 1 μm of the absorber close to the CdS layer is illuminated. Therefore, with this technique we are only probing the CdS/CdTe interface region.
Simulation of the solar cell parameters using current/voltage, capacitance/voltage and DLTS measurements was performed by means of the simulation package SCAPS. A thorough discussion of this program is given in [6] and [7].

3. Results and Discussion

3.1 General properties of the investigated CdS/CdTe thin film solar cells.
Prior to DLTS measurements the solar cells were characterised using capacitance/voltage (CV) and current/voltage (JV) measurements. Using CV measurements the doping density could be determined. For the vacuum activated cells a doping concentration of $1x10^{14}cm^{-3}$ was derived, for the air activated cells the doping concentration was somewhat higher: $4x10^{14}cm^{-3}$. Using JV measurements the solar cell characteristics were determined. The data is summarized in table 1.

3.2 Majority trap DLTS
Majority trap DLTS was performed on complete CdS/CdTe thin film solar cells, and both semi-shallow and mid-gap traps could be detected. These defects were already discussed in detail in a previous paper [3], therefore only the major results are given here. The signatures

and concentrations are listed in table 2 (hole traps H1-H7). The signatures of the defects are derived from the arrhenius diagram (figure 1). The mid-gap traps could be characterized using Isothermal DLTS (ITS), where the temperature is kept constant while the rate window is scanned. If we look at the concentrations of the detected defects it can be anticipated that the high concentration traps such as H5 and H7 will highly influence the cell's characteristics.

3.3 Electrical injection DLTS

Figure 2 shows the temperature scans for both kinds of samples, from 80 to 320K. In both cases a contribution of electron traps can be seen (negative bands) at high temperatures. These electron traps are located around mid-gap. However a complete characterization of these defect levels was not possible due to temperature limitations, even with ITS.

In vacuum activated cells no defect levels could be seen below 250K. In the air activated cells one electron trap, labelled E1, is detected. From the arrhenius diagram (figure 1) an activation energy of 0.44eV could be derived. The concentration is about 10^{11} cm^{-3}.

3.4 Optical DLTS

Another way to inject the junction with minority carriers is optical injection, which is done in optical DLTS (O-DLTS). Figure 3 shows the optical DLTS measurements of both kinds of samples.

If we look closer to these results some remarks can be made. First of all in both types of samples broad minority bands are visible around 150-200K. These minority signals are too broad to originate from a single defect. Some emission rate windows show a clear indication that two defects are present in the air activated cells. We designate them as E1* (which is the main peak) and E2* (which is visible as a shoulder of E1*). Even with extreme emission rate windows (0.45ms and 4500ms) we were unsuccessful in separating this large band into different components. This indicates that the activation energies of the defects are very closely spaced.

If we compare the electrical injection DLTS measurements with the O-DLTS measurements, it seems that E1 is identical to E1*. Subtracting both curves from each other and doing so for different emission rate windows we can construct an arrhenius diagram of E1* and E2* and extract a signature (figure 1 and table 2). E2* is located at 0.42eV below the conduction band, E1* is located 20meV deeper. Both defects have concentrations of about $5x10^{12}cm^{-3}$.

The situation is somewhat more complicated in the vacuum activated cells. We also see a broad minority trap around 200K, but till now we were unsuccessful in separating the components of the band. Probably it concerns closely spaced defects around 0.4eV below conduction band minimum. The concentrations are in the order of $10^{11}cm^{-3}$.

Secondly, no majority traps are detected in either sample using O-DLTS, not even the high concentrations of the mid-gap traps (hole traps H5, H6 and H7) which are visible in majority DLTS. There are two possible reasons for this. Maybe these defects are not present in the interface region. This seems unlikely because of their high concentration in the bulk of the solar cell. Another reason may be that these hole traps are also efficient electron traps. In such traps electron capture occurs more efficiently during the optical pulse. This implies that such traps are not occupied by holes during the pulse and as a result no emission of holes can be detected.

A final remark is the absence of minority peaks in the inj-DLTS measurements of the vacuum activated cells and the absence of E2* in the air activated cells. Two explanations are proposed. First of all there is a possibility that the defects detected close to the interface region are not present in the bulk layer of the junction. Second we have to take into account the importance of the back contact barrier which is present is these cells [9]. This barrier is

limiting the current in forward polarization so few electrons are injected into the junction, with no detection of minority traps as a result.

3.5 JV-measurements and SCAPS simulations

In this paragraph, we check if the deep level parameters deduced from the DLTS measurements are consistent with the measured dark J(V,T) curves.

In figure 4 the J(V) curve at 300 K is shown. The linear part of this curve (between 0.3 V and 0.6 V) can be fit with experimental parameters ($J_0 = 3.6\ 10^{-8}$ mA/cm^{-2} and ideality factor A = 1.25). Apart from the measured curve, also 3 different simulation results from SCAPS are presented [6], [7]. The data concerning the recombination centres for the 3 simulations is given in table 3. For other SCAPS simulation parameters, we refer to [10].

In the first simulation, the exact data is used (resulting from the DLTS measurement). The unknown values (σ_n for H7 and σ_p for E1 and E2) were chosen realistically. The resulting curve illustrates how only the deep levels E1 and E2 contribute to the recombination current. The shape of the curve can be described accurately with the current transport theory of Sah, Noyce and Shockley [11]. It predicts how the deep levels E1 and E2 realise a J(V) curve with A-factor smaller than 2 in the voltage region below 0.6 V. As can be seen, the shape corresponds already well to the measured J(V) curve, but the J-values are two orders of magnitude too low.

To realise a better correspondence between the measured and simulated curves, mainly the concentrations of the deep levels have to be increased (while the other parameters can be kept constant). The measured curve at low voltages suggests a contribution to the recombination current resulting from the midgap centre H7. This contribution is simulated with the parameters shown in the second case of table 3. In order to keep the deep donor concentration below the background shallow acceptor concentration (10^{14} cm^{-3}), the capture cross sections for H7 were increased to reach the correct magnitude for the recombination at low voltage. Second (as illustrated with the case 3), the concentrations of the centre E2 was increased to realise a good fit to the simulated curve. Furthermore in figure 5, the simulations were compared to the J(V,T) measurements.

Whether these high defect concentrations are realistic is still unclear. If we suppose that the DLTS concentrations are correct, the raise of the concentrations in our simulation to fit the experimental results is unjustified and a more complicated model needs to be developed. However, if we are looking at the success of simulations of the J(V,T) measurements, it is more plausible that the concentrations found with DLTS are to low. Indeed measurements with higher light intensities indicate a much higher defect concentration. This aspect needs further investigation.

4. Conclusion

Electrical injection DLTS and optical DLTS resulted in the detection of new minority traps in air activated and vacuum activated CdS/CdTe thin film solar cells. A signature could be derived for the defects in the air activated cells: two closely spaced defects are located at 0.42 and 0.44eV under the conduction band. The vacuum activated cells also contain electron traps in this energy region, but no signature could be derived yet. The concentrations are a few percent of the free carrier concentration in the air activated cells and even less in the vacuum activated samples.

Using SCAPS we could simulate the forward current characteristics of the solar cells using the defects detected with DLTS. The simulation results are in close agreement with the experimental results if the concentrations are taken sufficiently high.

5. Acknowledgements

This work was supported in part by the Research Fund (BOF) of Ghent University

6. References

[1] K. Zanio, Cadmium Telluride (Ser. Semiconductors and Semimetals, vol.13), Academic Press, New York-San Francisco-London, 1978.
[2] D. Bonnet, P. Meyers, J. Mater. Res. 13 (1998) 2740
[3] J. Versluys, P. Clauws, P. Nollet, S. Degrave and M. Burgelman, Thin Solid Films, 431-432, (2003), 148
[4] P. Nollet, M. Köntges, M. Burgelman, S. Degrave and R. Reineke-Koch, Thin Solid Films, 431-432, (2003), 414
[5] S. Weiss, R. Kassing, Solid State Electronics 31 (1982) 1733
[6] A. Niemegeers and M. Burgelman. In: proceedings of the 25nd IEEE Photovoltaic Specialists Conference, PVSC, 1996, p 901
[7] S. Degrave, M. Burgelman, P. Nollet, in: Proceedings of the third World Conference on Photovoltaic Solar Energy Conversion, Osaka, Japan, may 12-16, 2003, to be published
[8] T.H. Myers, S.W. Edwards, J.F. Schetzina, J. Appl. Phys. 52 (1981) 4231
[9] P. Nollet, M. Burgelman, S. Degrave, J. Beier, in: Proceedings of the 29th IEEE Photovoltaic Specialists Conference, PVSC, 2002, p 704
[10] M. Köntges, R. Reineke-Koch, P. Nollet, J. Beier, R. Schäffler, J. Parisi, Thin Solid Films, 403-404, (2002), 280
[11] C.T. Sah, R. N. Noyce, and W. Shockley, Proceedings of the IRE, 45 (1957) 1228

Reference number of Manuscript: D-II.4

List of figure captions

Figure 1: Arrhenius plot of deep levels in CdS/CdTe solar cells. The signatures are given in table 2. H1-H7: hole traps found with normal DLTS, E1: electron trap found with electrical injection DLTS, E1* and E2* electron traps found with optical DLTS.

Figure 2: Electrical injection DLTS of CdS/CdTe thin film solar cells. Reverse bias = -1V; pulse height = 1.5V; fill pulse = 1ms; emission rate window = 4.5ms.

Figure 3: Optical DLTS of CdS/CdTe TF solar cells. Reverse bias = -1V; fill pulse = 10ms; wavelength = 635nm, illumination through front contact.

Figure 4: Measured J(V) curve (squares) and SCAPS simulations (lines). The difference between the 3 SCAPS simulations are the deep recombination centres (see table 3).

Figure 5: Temperature dependent J(V,T) measurements (symbols) compared with simulations (lines).

Table 1: Solar cell characteristics derived from JV-measurements.

Table 2: Signature and concentration of deep levels in CdS/CdTe cells, as determined by DLTS. (E_T,K_T) is the signature of the defect levels, originating from $e_{n,p}=K_T T^2 \exp(-E_T/kT)$, N_T is trap concentration.

Table 3: Parameter values used in the simulations (- means that the parameter value is kept unchanged compared to the previous case). Shallow doping concentration CdTe: $10^{14}cm^{-3}$, H7 was simulated as donor, E1 and E2 as acceptors).

Reference number of the paper: D-II.4

Table 1
Solar cell characteristics derived from JV-measurements

	J_{SC}	V_{OC}	FF (%)	η (%)
Vacuum activated	21.2	790	61	10.95
Air activated	21.3	785	67	11.30

Reference number of the paper: D-II.4

Table 2

Signature and concentration of deep levels in CdS/CdTe cells, as determined by DLTS. (E_T,K_T) is the signature of the defect levels, originating from $e_{n,p}=K_T T^2 \exp(-E_T/kT)$, N_T is trap concentration.

	E_T (eV)	K_T ($s^{-1} K^{-2}$)	N_T (cm^{-3})	activation	Method
H1	0.113 (±0.002)	$1.2(\pm0.5)\times10^{8}$	3.3×10^{12}	air	DLTS
H2	0.185 (±0.005)	$1.2(\pm1.1)\times10^{13}$	2.3×10^{12}	air	DLTS
H3	0.126 (±0.001)	$9.3(\pm2.5)\times10^{7}$	1.3×10^{11}	vacuum	DLTS
H4	0.502 (±0.009)	$1.8(\pm0.9)\times10^{9}$	2.8×10^{11}	vacuum	DLTS
H5	0.741 (±0.020)	$4.8(\pm4.4)\times10^{10}$	3.6×10^{12}	vacuum	ITS
H7	0.717 (±0.014)	$1.5(\pm0.8)\times10^{5}$	4.5×10^{13}	air	ITS
E1	0.441 (±0.012)	$2.2(\pm1.8)\times10^{7}$	3.6×10^{11}	air	Inj-DLTS
E1*	0.441 (±0.012)	$2.2(\pm1.8)\times10^{7}$	5.6×10^{12}	air	O-DLTS
E2*	0.421 (±0.017)	$5.8(\pm3.6)\times10^{8}$	4.1×10^{12}	air	O-DLTS

Reference number of the paper: D-II.4

Table 3

Parameter values used in the simulations (- means that the parameter value is kept unchanged compared to the previous case). Doping concentration CdTe: $10^{14}cm^3$, H7 was simulated as donor, E1 and E2 as acceptors)

	Case 1: Exact DLTS data	Case2: Midgap level	Case 3: Deep acceptors
H7 (E_V+0.72 eV)			
N_t [cm^{-3}]	$4.5\ 10^{13}$	-	-
σ_p [cm^2]	$7.5\ 10^{-17}$	$7.5\ 10^{-14}$	-
σ_n [cm^2]	10^{-15}	$4\ 10^{-12}$	-
E1 (E_C-0.44 eV)			
N_t [cm^{-3}]	$5.6\ 10^{12}$	-	-
σ_n [cm^2]	$7\ 10^{-14}$	-	-
σ_p [cm^2]	10^{-11}	-	-
E2 (E_C-0.42 eV)			
N_t [cm^{-3}]	$4.1\ 10^{12}$	-	10^{15}
σ_p [cm^{-3}]	$1.2\ 10^{-12}$	-	-
σ_p [cm^{-3}]	10^{-12}	-	-

Reference number of the paper: D-II.4

Fig. 1.

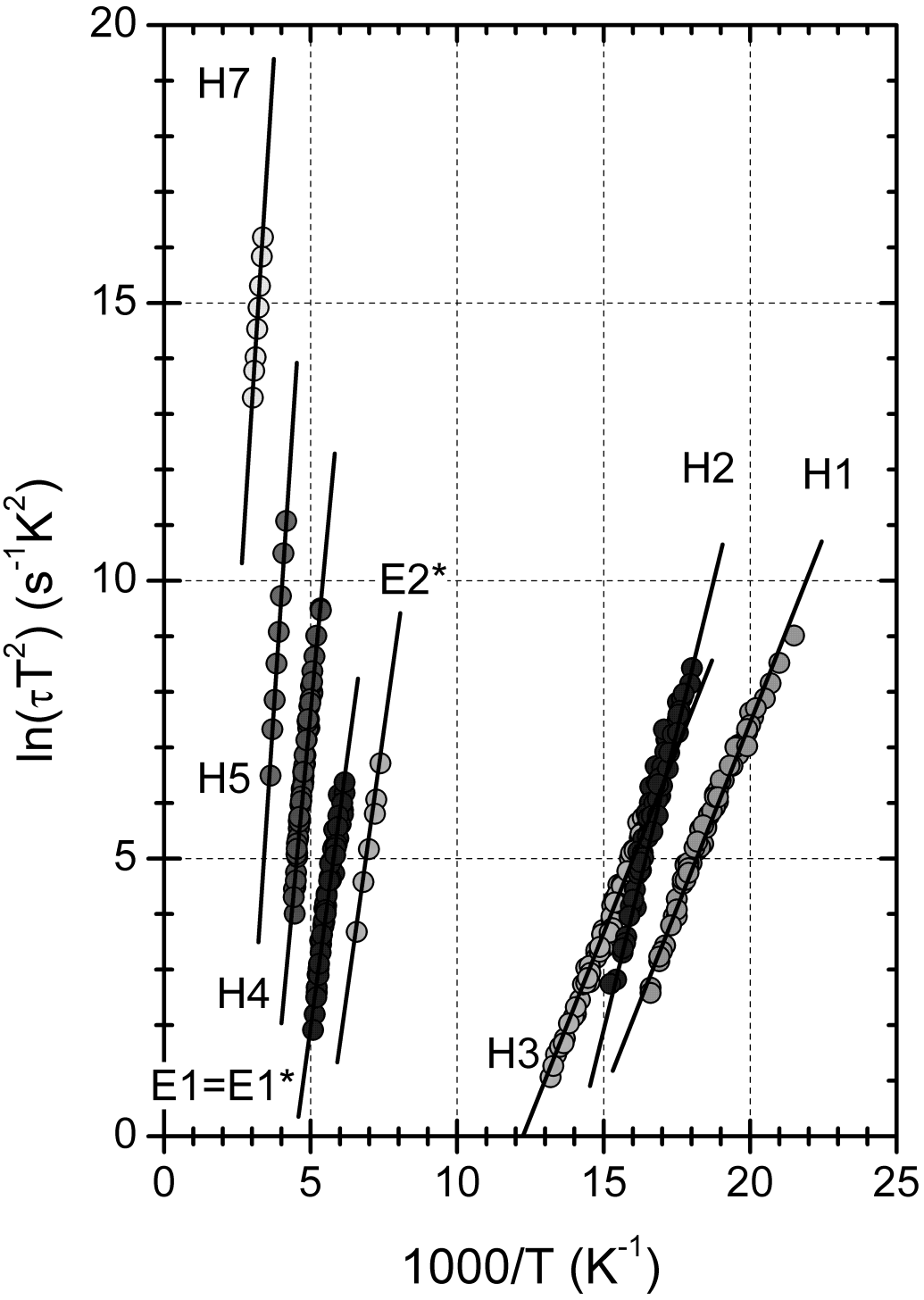

Reference number of the paper: D-II.4
Fig. 2.

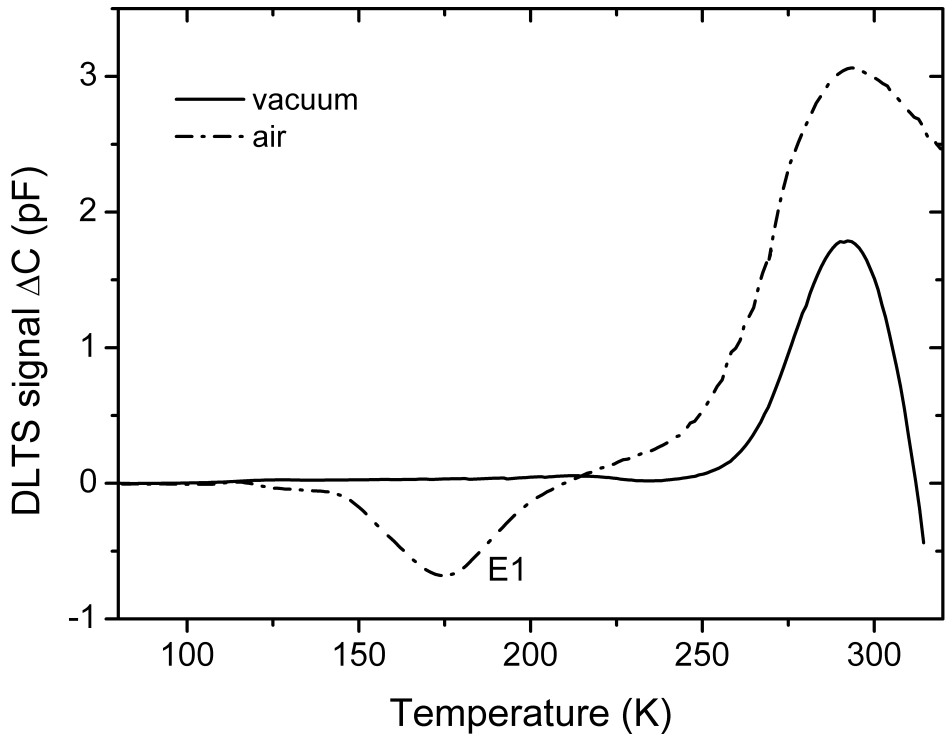

Reference number of the paper: D-II.4
Fig. 3.

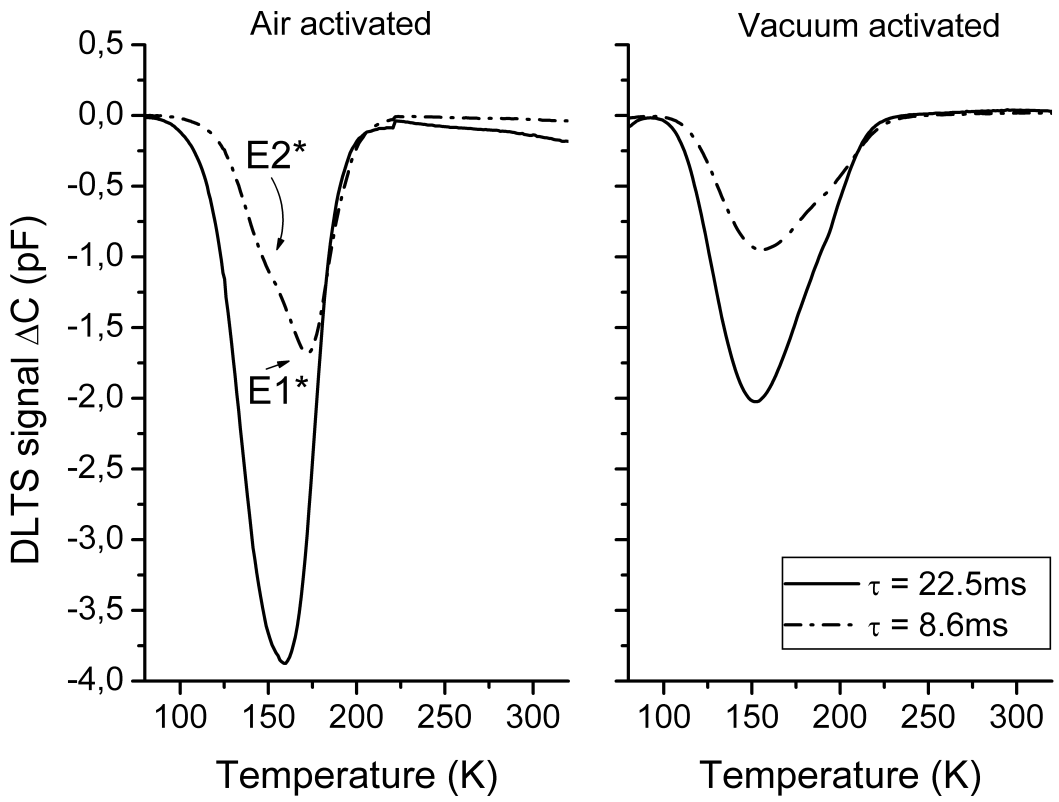

Reference number of the paper: D-II.4

Fig. 4.

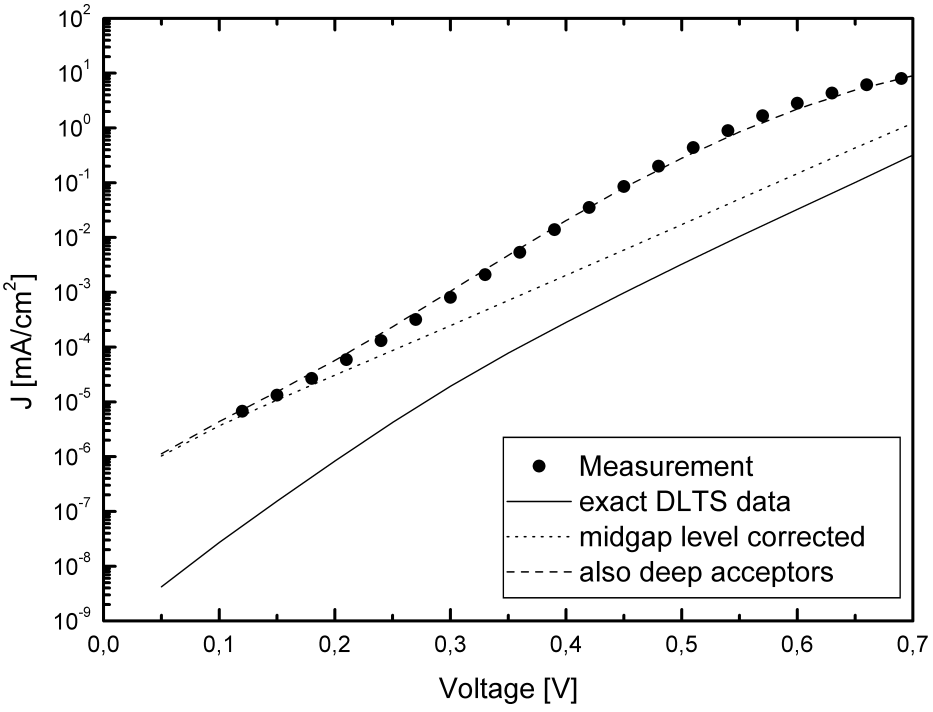

Reference number of the paper: D-II.4

Fig. 5.